

# A Physiological Information Extraction Method Based on Wearable PPG Sensors with Motion Artifact Removal

Wei-Jheng Lin and Hsi-Pin Ma

Department of Electrical Engineering, National Tsing Hua University, Hsinchu, Taiwan

Email: leolin651@gmail.com, hp@ee.nthu.edu.tw

**Abstract**—In this paper, a method to extract physiological information from Photoplethysmography (PPG) signal with motion artifact detection and removal is proposed. First, PPG data recorded from wearable sensors are pre-processed by discrete wavelet transform to remove unwanted noise and extract AC/DC component. Then, the characteristic points such as peaks and troughs are identified for feature extraction and physiological information extraction. To detect the motion artifact periods, we use support vector machine (SVM) for classification. The detection performance was verified by PPG signals from 11 different healthy subjects. The proposed method operates in 7 seconds with accuracy of 94.4%, sensitivity of 90.35%, and specificity of 99.36%. The motion artifact removal is accomplished by Kalman filter to track the SpO<sub>2</sub> and heart rate (HR) extracted from motion artifact-corrupted periods. The parameters of Kalman filter are determined by the detection results. In the case of waving hand left-right, the average mean absolute bias of artifact-corrupted SpO<sub>2</sub> and HR are 1.34% and 7.29 bpm, respectively. After applying the algorithm, the bias becomes 0.8% and 4.29 bpm. In the case of waving hand up and down, the errors of SpO<sub>2</sub> and HR reduce from 1.31% to 0.82% and 13.97 bpm to 6.87 bpm.

**Index Terms**—PPG, motion artifact, discrete wavelet transform, support vector machine, Kalman filter

## I. INTRODUCTION

Photoplethysmography (PPG) is a non-invasive and low-cost technique widely used either in clinical applications or in-home care. These applications usually require analysis on the amplitude, rhythm, and peripheral pulse of PPG signals. The main applications of the PPG are calculations of the arterial oxygen saturation and heart rate (HR). For example, PPG signals were found to be useful for detection and diagnosis of cardiac arrhythmias [1] [2]. In addition, the oxygen saturation drop can be treated as a syndrome of sleep apnea patients. Moreover, since the PPG resulting waveform also contains the venous or complex mixture of influences, new applications of PPG signals have been proposed. The calculation of blood pressure and respiration rate are two examples. However, to extract correct physiological information, the PPG signal is required to be clean. Thus, there is high demand for effectively extract reliable physiological information from motion corrupted PPG signals. Several approaches have been proposed

to reduce motion artifact including independent component and adaptive filtering [3] [4] [5]. Hence, an approach for extracting the reliable physiological information from motion corrupted PPG signal is proposed in this paper. This approach is composed of three part: physiological information extraction, motion artifact detection, and motion artifact removal.

The remainder of the paper is organized as follows: Section II introduces the proposed signal pre-processing and physiological information extraction method, including the SpO<sub>2</sub> and heart rate extraction. Section III explains the approach to detect motion artifact by support vector machine (SVM) and to remove motion artifact effect on physiological information by Kalman filter. The result of the motion artifact detection and motion artifact removal are given in Section IV. Finally, our works are concluded in Section V.

## II. SIGNAL PREPROCESSING AND PHYSIOLOGICAL INFORMATION EXTRACTION

### A. PPG Signal Processing Based on DWT

Discrete wavelet transform (DWT) is derived from continuous wavelet transform (CWT), with the concept of filter banks to accomplish multi-resolution analysis. Comparing with CWT, DWT utilizes filtering and down-sampling processes to achieve low computational complexity. Since wavelet analysis is an efficient method for data compression and noise reduction, especially for non-stationary signal, DWT is selected as the signal processing tool in the proposed scheme.

DWT is used to de-noise and separate the AC and DC components of PPG signal before physiological information extraction. The sampling rate of the PPG raw data is 200 Hz. In the DWT process, the PPG signal is first decomposed. Then, the signal components in the bandwidth of 0.39-12.5 Hz (level 4 to level 8) are reconstructed. Besides, the universal threshold [6] is setting in level 4 to remove the noisy components by using soft thresholding method. The wavelet base which used in the process is Daubechies wavelet base because it can restore the peak-to-peak amplitude of PPG signal [7].

### B. SpO<sub>2</sub> and HR Extraction

The most common method to measure SpO<sub>2</sub> in pulse oximeter is the *ratio to ratio* technique [8]. The technique extracts the AC and DC parts from infrared (IR) and red PPG

This research is supported in part by the Ministry of Science and Technology, Taiwan, R.O.C. under Grants MOST104-2220-E-007-003-, MOST104-2220-E-007-019-, and MOST104-3115-E-007-002-. We also thank the experiment resource and facility support from DigiO2 International Co., Ltd.

signals, and calculate the R value, as

$$R = \frac{AC_{red}/DC_{red}}{AC_{infrared}/DC_{infrared}} \quad (1)$$

The  $AC_{red}$  and  $DC_{red}$  denote the AC and DC magnitude of red PPG signal, respectively. The  $AC_{infrared}$  and  $DC_{infrared}$  represent the AC and DC magnitude of IR PPG signal, respectively. The  $SpO_2$  is computed by the empirical linear approximation equation, as

$$SpO_2\% = (110 - R)\% \quad (2)$$

The AC component of PPG is caused by the cardiac cycle and thus the PPG can be a source of heart rate information. Therefore, heart rate can be extracted from peak-to-peak interval of two successive pulses of PPG.

### III. PROPOSED APPROACHES FOR MOTION ARTIFACT DETECTION AND REMOVAL

#### A. Motion Artifact Detection

Since the motion artifact distorts the PPG signals, the waveform morphology of PPG segments corrupted by motion artifacts differs from that of clean segments. Therefore, to identify the corrupted PPG segments, some meaningful features must be extracted from PPG signals. After the features are extracted, support vector machine (SVM) is selected as the classifier to distinguish the corrupted segments by motion artifacts according to the extracted features. The block diagram for motion artifact detection is shown in Figure 1. The PPG signal is pre-processed by the method mentioned in Section II, then the features from training data are extracted and normalized. The SVM model is then trained according to the features from training data.

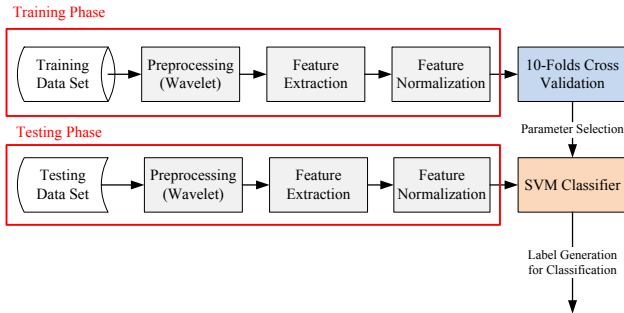


Fig. 1. The block diagram for motion artifact detection.

1) *Feature Extraction*: The features which are used to detect motion artifact include standard deviation of peak-to-peak amplitudes, mean absolute deviation of peak-to-peak amplitudes, standard deviation of peak-to-peak intervals, and the kurtosis.

- **Standard Deviation of Peak-to-Peak Amplitude**

The standard deviation (SD) measures the amount of variation from the average. A low standard deviation

value means that the data is close to the mean value. A high standard deviation value means that data are more spread from mean value. The standard deviation of peak-to-peak amplitude is chosen as the feature to detect corrupted PPG segments by motion artifacts. It is defined by:

$$SD_{AMP,n} = \sqrt{\frac{1}{N} \sum_{i=1}^N (A_{n,i} - \bar{A}_n)^2} \quad (3)$$

where  $A_{n,i}$  is the peak-to-peak amplitude of  $i$ th pulse in the  $n$ th segment of PPG signals.  $\bar{A}_n$  is the mean of peak-to-peak amplitude in  $n$ th segment.

- **Mean Absolute Deviation of Peak-to-Peak Amplitude**  
Mean absolute deviation (MAD) is the average of the absolute deviations from a central point. MAD is a method for measuring variability. The MAD value can be defined after peak-to-peak amplitude of pulses are calculated in  $n$ th segment.

$$MAD_n = \sum_{i=1}^N \frac{|A_{n,i} - \bar{A}_n|}{N} \quad (4)$$

The symbols above are the same as the symbols used in the  $SD_{AMP,n}$ .

- **Standard Deviation of Peak-to-Peak Interval**  
The pulse-to-pulse intervals are derived by computing the difference between two successive peak times. The standard deviation of pulse-to-pulse intervals is defined as:

$$SD_{PPI,n} = \sqrt{\frac{1}{N} \sum_{i=1}^N (T_{n,i} - \bar{T}_n)^2} \quad (5)$$

where  $T_{n,i}$  is the peak time of  $i$ th pulse in  $n$ th segment of PPG signals.  $\bar{T}_n$  is the mean of pulse-to-pulse intervals in  $n$ th segment.

- **Kurtosis**

Kurtosis is a measure of the peakedness of the probability distribution or distribution of samples. The kurtosis of a distribution is defined as:

$$Kurtosis = \frac{E(x - \mu)^4}{\sigma^4} \quad (6)$$

where  $\mu$  is mean of variables  $x$ ,  $\sigma$  is the standard deviation of  $x$ . High kurtosis tends to have a distinct peak near the mean, while low kurtosis tends to have a flat top near the mean rather than a sharp peak. The kurtosis is measured much higher in magnitude for corrupted segments by motion artifacts, while the clean segments is much lower in magnitude [9] [10]. Thus, the kurtosis is chosen as a candidate of the features.

2) *Support Vector Machine*: Support vector machine (SVM) is a machine learning method that can separate all data points into two classes. The aim of SVM is to find the best separating hyperplane that separates all data points of one class from those of the other class. SVM is a powerful classifier that is widely used in classification, regression and pattern recognition due to its high accuracy and robustness

[11]. In the proposed scheme, we employ linear SVM classifier in order to reduce the computational complexity. In this paper, 10-folds cross-validation is selected to train the SVM model.

### B. Motion Artifact Removal

Since the value of SpO<sub>2</sub> and HR extracted from PPG signal may be corrupted by the motion artifacts, the recording of SpO<sub>2</sub> and HR would be unreliable. As a result, our strategy to solve the problem is to use Kalman filter to correct the abnormal recordings of SpO<sub>2</sub> and HR which are resulted from the motion artifacts.

1) *Introduction to Kalman Filters:* The Kalman filter (KF) is an optimal state estimation method that uses a series of noisy measurements observed over time to generates estimates of unknown states. In Kalman filtering algorithm, the controlled process,  $x$  is governed by the linear stochastic difference equation:

$$x_k = Ax_{k-1} + Bu_{k-1} + w_{k-1} \quad (7)$$

with a measurement  $z$  that is:

$$z_k = Hx_k + v_k \quad (8)$$

The random variables  $w_k$  and  $v_k$  are the process and measurement noise that are assumed to be independent, white, and with normal probability distributions,  $p(w) \sim N(0, Q)$  and  $p(v) \sim N(0, R)$ , respectively.

The matrix  $A$  in (7) is the state transition matrix that relates the state at the previous state  $x_{k-1}$  to the current state  $x_k$ . The matrix  $B$  is the optional control-input model for the control input  $u_k$  that relates to the state  $x_k$ . In the measurement (8), the matrix  $H$  relates to the measurement  $z_k$ .

The Kalman filtering algorithm can be fall into two parts: (1) time update equations, and (2) measurement update equations.

Time update equations:

$$\hat{x}_k^- = A\hat{x}_{k-1} + Bu_{k-1} \quad (9)$$

$$P_k^- = AP_{k-1}A^T + Q \quad (10)$$

Measurement update equations:

$$K_k = P_k^- H^T (HP_k^- H^T + R)^{-1} \quad (11)$$

$$\hat{x}_k = \hat{x}_k^- + K_k(z_k - H\hat{x}_k^-) \quad (12)$$

$$P_k = (I - K_k H)P_k^- \quad (13)$$

$\hat{x}_k^-$  represents the *a priori* state estimate at the current time step before a given measurement  $z_k$ , and  $\hat{x}_{k-1}$  is the *a posteriori* state estimate from the previous time step after a given measurement  $z_{k-1}$ .  $P_k^-$  and  $P_{k-1}$  are the error covariance of *a priori* and *a posteriori* estimate corresponding to the current time step and the previous time step, respectively. In (11), the Kalman gain,  $K_k$  is computed first during the measurement update. The Kalman gain is required to minimize

the *a posteriori* error covariance,  $P_k$ . Overall, the process of Kalman filtering algorithm is repeated with the previous *a posteriori* estimates used to predict the new *a priori* estimates.

2) *Kalman Filtering Initialization and Operation for SpO<sub>2</sub> Correction:* For SpO<sub>2</sub> correction, we apply the Kalman filter to track the R value. According to the evident that the sudden SpO<sub>2</sub> value would not increase or decrease between successive beats over 2% [12], the R value changes not significantly between successive beats. Thus the R value at each beat is assumed to be approximately equal to the next beat. Therefore, The parameter  $A$  which is related to the system state is set to 1. Furthermore, we assume there is no control input ( $B=0$ ), and noisy measurement is directly observed ( $H=1$ ). Here, we presumed that we have a very small process variance,  $Q = 1 \times 10^{-4}$ . And the initial value for  $P_{k-1}$  can be chosen as any positive since it would eventually converge. We select the initial value  $P_{k-1} = 1$ .

The measurement noise covariance  $R$  is usually measured before utilizing the filter. For the clean signal, the measurement noise is measured by comparing the R value generated from the reference pulse oximeter tester. We assume that the tester generates the physiological information correctly, thus the measurement error between the measurement by our method and the reference value by the tester can be seen as the the measurement noise. The standard deviation from mean value is supposed to be the measurement noise. However, the standard deviation may diverse because of different perfusion and transmission condition, thus we selected the average value 1.75 as the measurement noise. The measurement noise of R value for artifact-free signal is 0.07, and the measurement noise covariance  $R$  is 0.0049. However, the measurement noise for corrupted signal by motion artifacts was difficult to measure, thus we compared the standard deviation between reference and the corrupted R value in the same period. We found that the average standard deviation of the corrupted period was about 2.8 times as large as the reference. So, the measurement noise covariance  $R$  is selected as 0.04 for corrupted period.

3) *Kalman Filtering Initialization and Operation for HR Correction:* The parameters used to track HR are the same as those in correcting SpO<sub>2</sub>, except for measurement noise covariance  $R$  and process noise covariance  $Q$ . Estimating the measurement noise for clean signal is as well as the method used in SpO<sub>2</sub>. The measurement noise covariance  $R$  for artifact-free is set as 41 bpm<sup>2</sup>. The process noise covariance is determined by the evident that the interval between successive heart beats exceeds 50 ms is the critical threshold for distinguishing physiological and pathological states [13]. Thus, we supposed that the difference of interval between successive heart beats would not exceeds 50 ms, meaning that the deviation of the process is 3 bpm. Therefore, the process noise covariance  $Q$  is set as 9 bpm<sup>2</sup>. For motion-corrupted period, the measurement noise  $R$  is estimated as 308 bpm<sup>2</sup>.

The filter parameters are listed as Table I:

TABLE I  
PARAMETERS FOR KALMAN FILTER TRACKING.

	R value	HR
A	1	1
B	0	0
H	1	1
P <sub>0</sub>	1	1
Q	$1 \times 10^{-4}$	9
R	0.0049 for clean period 0.04 for corrupted period	41 for clean period 308 for corrupted period

#### IV. EXPERIMENTAL SETTING AND RESULTS

In this section, the wearable PPG sensor which is used in the experiment is introduced. Besides, the experimental setting which used to verified the performance of PPG motion artifact detection and removal is represented.

##### A. Wearable PPG Sensor

The wearable transmission type PPG sensor was provided by DigiO2 (DigiO2 International Co., Ltd.). The sensor emits light with red light and infrared. The data can be transmitted by Bluetooth to the smart phone or the computer. The data transmission baud rate is 115.2 kbps.

##### B. Experimental Setting

Eleven healthy subjects were asked to sit down and wear two identical transmission type PPG sensors on their left and right index finger, respectively. The sensor attached on the left index finger was held in a stable position to get a reference signal as standard. The motion artifacts were induced by moving the sensor that attached on the right index finger. The movements that subjects were instructed to do includes waving hand left and right, waving hand up and down. In both of the cases, the subjects wave their right hand. Each motion is repeated 1 to 2 times in one second.

Each subject was asked to keep stationary for 1 minute for recording the clean data, and then be instructed to wave hand left and right for 1 minute. After the motion, subjects were asked to keep stationary for 1 minute again. For experimental setting of waving hand up and down was the same as the case of waving hand left and right. Each experiment was repeated two times per subject.

##### C. Results of Motion Artifact Detection

###### 1) Optimization of Regularization Parameters of SVM:

For linearly non-separable SVM, the tunable parameter is  $C$ . This parameter can determine the margin of decision bound and the tolerance of misclassified data. Therefore,  $C$  is an critical parameter when training the SVM model. We use 10-folds cross-validation and grid search method to select the parameters. The results is shown in Table II. We extracted the features from each segment of 7-second length, and applied different  $C$  to find the one with best accuracy. Experiment result shows that the best performance is selected when  $C$  is 1.

TABLE II  
GRID SEARCH FOR THE PARAMETER  $C$  OF LINEAR SVM.

$C$	Accuracy (%)
$2^{-5}$	85.61
$2^{-4}$	86.91
$2^{-3}$	87.31
$2^{-2}$	88.51
$2^{-1}$	91.41
1	94.41
$2^1$	92.51
$2^2$	92.11
$2^3$	92.21
$2^4$	92.21
$2^5$	92.11

2) *Results of Segment Length for Detection:* Because the classification features are statistical measurements, the segment length will affect the performance of classification. In the evaluation, the segment lengths are chosen from 3 sec to 9 sec. The classification performance for each segment length are listed in Table III. In all the cases, the results are derived from ten times 10-folds cross-validation. We find that the optimal classification accuracy is obtained when the segment length is 7 sec. At the segment length of 7 sec, the accuracy, sensitivity, and specificity are 94.40%, 90.35%, and 99.36%, respectively.

##### D. Results of Motion Artifact Removal

The improvement of SpO<sub>2</sub> and HR after Kalman filter tracking is shown in Table IV and V. The SpO<sub>2</sub> and HR are calculated every beat of 1 minute motion-corrupted data before and after Kalman filter tracking. The results show that the method can decrease the bias of both SpO<sub>2</sub> and HR. For finger clip sensor, the motion (such as waving hand) does not affect much on the range of SpO<sub>2</sub> value with the proposed signal pre-processing and SpO<sub>2</sub> extraction method. However, the results of heart rate extraction by beat-to-beat interval is sensitive to motion.

##### E. Comparison

The comparison between motion artifact detection with other studies are listed in Table VII. It can be seen that the detection accuracy of our work is similar to the other studies. There is one thing particularly noticeable is that the specificity of our work is higher than the others. The higher specificity means that the false alarm occur less frequently.

For the comparisons of motion artifact removal, the results are listed in Table VIII. In the table, the results are compared by mean bias and mean absolute bias. The bias of the SpO<sub>2</sub> and HR without motion artifact removal are denoted by mean bias (Orig.) and mean absolute bias (Orig.). The bias of the SpO<sub>2</sub> and HR with motion artifact removal are denoted by mean bias (Enh.) and mean absolute bias (Enh.). Our bias values are the average value which computed from every heart beat in 1 minute motion period for each subject. The value of [5] applies their algorithm in 6 healthy subjects with motion artifacts induced by running and walking. Their algorithm is based on adaptive filter, and the reference noise is

TABLE III  
DIFFERENT SEGMENT LENGTH WITH THEIR CORRESPONDING PERFORMANCE (MEAN $\pm$ SD).

Segment length (sec)	3	5	7	9
Accuracy (%)	87.60 $\pm$ 2.08	90.67 $\pm$ 2.26	94.40 $\pm$ 1.85	89.92 $\pm$ 3.03
Sensitivity (%)	80.28 $\pm$ 2.18	83.40 $\pm$ 4.62	90.35 $\pm$ 3.10	84.15 $\pm$ 4.68
Specificity (%)	93.88 $\pm$ 3.94	96.82 $\pm$ 1.78	99.36 $\pm$ 1.07	96.03 $\pm$ 2.89

TABLE IV  
COMPARISON OF SpO<sub>2</sub> AND HR ACHIEVED BEFORE AND AFTER KALMAN FILTER TRACKING IN VERTICAL HAND MOVEMENT CASE. THE VALUES IN THE TABLE IS MEAN ABSOLUTE BIAS.

	SpO <sub>2</sub> (Orig.)	SpO <sub>2</sub> (KF)	HR (Orig.)	HR (KF)
Subject 1	1.02	0.98	10.39	4.23
Subject 2	0.80	0.63	9.76	8.31
Subject 3	0.58	0.45	24.17	8.02
Subject 4	0.78	0.31	23.73	16.48
Subject 5	0.81	0.45	6.96	2.66
Subject 6	0.78	0.32	20.73	10.28
Subject 7	0.79	0.68	16.44	4.74
Subject 8	1.21	1.06	12.91	6.46
Subject 9	1.98	0.58	13.58	8.80
Subject 10	1.17	0.92	10.73	3.75
Subject 11	2.81	2.71	4.27	1.89

TABLE V  
COMPARISON OF SpO<sub>2</sub> AND HR ACHIEVED BEFORE AND AFTER KALMAN FILTER TRACKING IN HORIZONTAL HAND MOVEMENT CASE. THE VALUES IN THE TABLE IS MEAN ABSOLUTE BIAS.

	SpO <sub>2</sub> (Orig.)	SpO <sub>2</sub> (KF)	HR (Orig.)	HR (KF)
Subject 1	0.53	0.15	5.76	2.28
Subject 2	1.24	0.57	5.22	3.95
Subject 3	0.51	0.19	5.06	2.66
Subject 4	1.05	0.8	10.02	6.54
Subject 5	0.29	0.08	2.18	0.88
Subject 6	1.54	0.91	9.52	5.32
Subject 7	4.64	2.75	7.02	3.37
Subject 8	0.83	0.79	15.12	9.24
Subject 9	0.47	0.24	10.49	7.29
Subject 10	0.66	0.26	7.25	3.45
Subject 11	2.97	2.16	2.52	2.22

generated by model based method. The performance is better than us but they do not deal with motion artifact detection. For [14], they proposed an approach based on singular spectrum analysis (SSA), a blind source separate method to remove motion artifacts. In this study. Their algorithm provides better results than ours and [5] but the computation complexity is much higher because SSA is an iterative approach. Thus, it is suitable for offline data analysis. For the adaptive filter algorithm in [5], the computational complexity is relatively low compare with the SSA method. For our methods, the computational complexity of Kalman filter is  $O(k^{2.4})$ ,  $k$  is the dimension of measurement. In comparison to adaptive filter, the computational complexity is higher than traditional LMS adaptive filter because the Kalman filtering process involves the inverse matrix computation. However, in our assumption the parameters are 1 dimension, so there are no inverse matrix computation in the operation of Kalman filter. Moreover, the approach in [5] requires to compute the reference noise for

adaptive noise cancellation, the computational complexity is much higher than the adaptive noise cancellation with known reference noise. Besides, our method is not necessary to compute every samples. The Kalman filter is operated every heart beat.

The Kalman filtering algorithm is coded with MATLAB (2012a) on an Intel Core i5 3.6 GHz. For 1 minutes PPG data, it took 4.57 ms for SpO<sub>2</sub> correction and 2.82 ms for HR correction. The computational complexity of our work is listed in Table VI, including DWT and Kalman filtering. The DWT is based on convolution computation. The SVM classification is not listed because it is hard to incorporate high dimension knowledge.

TABLE VI  
THE COMPUTATIONAL COMPLEXITY OF DWT AND KALMAN FILTER

Algorithm	DWT	Kalman filter
Complexity	$O(2NL)$	$O(k^{2.4})$

$N$  is the number of filter tap  
 $L$  is the number of number of decomposition level  
 $k$  is the dimension of measurement

## V. CONCLUSION

In this paper, we proposed a method to extract physiological information from PPG signal with motion artifact detection and removal. To extract the reliable features that are used to detect the motion artifacts, discrete wavelet transform (DWT) based de-noising is applied to do the signal pre-processing before detection and artifact removal. The support vector machine is selected as the motion artifact detector due to its robustness. The parameters of SVM model are optimized by using 10-fold cross-validation. The best detection segment length of 7-second for our detection method is also verified. The proposed detector can provide accuracy of 94.4%, sensitivity of 90.35%, and specificity of 99.36% with 7-second segment length.

In addition, the motion artifact removal method is also proposed. Instead of reconstructing the PPG signal, we use Kalman filter to correct the unreliable recording of SpO<sub>2</sub> and HR due to motion artifact. By tuning the parameters of filter according to the detection results, the SpO<sub>2</sub> and HR can be estimated from contaminated signal and the reading can be stabilized. The results of Kalman filter tracking show that the average mean absolute bias can be reduced to 0.8% and 4.29 bpm in comparison with original (1.34% and 7.29 bpm) in the case of waving hand left and right. In the case of waving hands up and down, the errors of SpO<sub>2</sub> and HR can be reduced from 1.31% to 0.82% and 13.97 bpm to 6.87 bpm.

TABLE VII  
COMPARISON OF MOTION ARTIFACT DETECTION WITH RELATED WORKS.

	This work	J. W. Chong [15]	R. Krishnan [9]
Sensor mode	Transmission	Reflectance	Reflectance
Subject	11 healthy subjects	9 healthy subjects	10 healthy subjects
Motion type	Hand movement	Finger movement	Hand movement
Detector	Linear SVM	Linear SVM	Neyman–Pearson detection rule
Segment length	7 s	7 s	2–3 s
Accuracy (%)	94.4	94.4	96
Specificity (%)	99.36	94.7	N/A
Sensitivity (%)	90.35	94.7	N/A

TABLE VIII  
COMPARISON OF MOTION ARTIFACT REMOVAL WITH RELATED WORKS.

	This work	[5]	[14]
Sensor type	Transmission	Transmission	Reflectance
Subject	11 healthy subjects	6 healthy subjects	9 healthy subjects
Motion type	Hand motion	Run & walk	Finger motion
Functionality	Detection/Reduction	Reduction	Reduction
Comparison of SpO <sub>2</sub> (%)			
Mean Bias (Orig.)	-1.15	-1.8	N/A
Mean Bias (Enh.)	0.21	0.15	N/A
Mean Abs Bias (Orig.)	1.33	6.9	N/A
Mean Abs Bias (Enh.)	0.81	0.6	N/A
Comparison of Heart rate (bpm)			
Mean Bias (Orig.)	1.28	-2.3	8.09
Mean Bias (Enh.)	0.52	0.36	0.19
Mean Abs Bias (Orig.)	10.63	8.7	N/A
Mean Abs Bias (Enh.)	5.58	2.1	N/A

In conclusion, the study provides a method to extract SpO<sub>2</sub> and HR for PPG signal with motion artifact detection and removal. Because the detector is based on machine learning algorithm, it is able to apply to unknown data via some training. Besides, due to the simple computation of Kalman filter, it is able to run online.

## REFERENCES

- [1] V. F. Blanc, M. Haig, M. Troli, and B. Sauvé, “Computerized photoplethysmography of the finger,” *Canadian Journal of Anaesthesia*, vol. 40, no. 3, pp. 271–278, 1993.
- [2] A. A. Awad, M. A. M. Ghobashy, R. G. Stout, D. G. Silverman, and K. H. Shelley, “How does the plethysmogram derived from the pulse oximeter relate to arterial blood pressure in coronary artery bypass graft patients?” *Anesthesia & Analgesia*, vol. 93, no. 6, pp. 1466–1471, 2001.
- [3] B. S. Kim and S. K. Yoo, “Motion artifact reduction in photoplethysmography using independent component analysis,” *IEEE Transactions on Biomedical Engineering*, vol. 53, no. 3, pp. 566–568, 2006.
- [4] H. H. Asada, H.-H. Jiang, and P. Gibbs, “Active noise cancellation using MEMS accelerometers for motion-tolerant wearable bio-sensors,” in *IEEE International Conference on Engineering in Medicine and Biology Society*, vol. 1, 2004, pp. 2157–2160.
- [5] R. Yousefi, M. Nourani, S. Ostadabbas, and I. Panahi, “A motion-tolerant adaptive algorithm for wearable photoplethysmographic biosensors,” *IEEE Journal of Biomedical and Health Informatics*, vol. 18, no. 2, pp. 670–681, 2014.
- [6] D. Donoho, “De-noising by soft-thresholding,” *IEEE Transactions on Information Theory*, vol. 41, no. 3, pp. 613–627, May 1995.
- [7] M. Raghuram, K. Madhav, E. Krishna, and K. Reddy, “On the performance of wavelets in reducing motion artifacts from photoplethysmographic signals,” in *IEEE International Conference on Bioinformatics and Biomedical Engineering (iCBBE)*, 2010, pp. 1–4.
- [8] J. A. Pologe, “Pulse oximetry: technical aspects of machine design,” *International Anesthesiology Clinics*, vol. 25, no. 3, pp. 137–153, 1987.
- [9] R. Krishnan, B. Natarajan, and S. Warren, “Two-stage approach for detection and reduction of motion artifacts in photoplethysmographic data,” *IEEE Transactions on Biomedical Engineering*, vol. 57, no. 8, pp. 1867–1876, 2010.
- [10] N. Selvaraj, Y. Mendelson, K. H. Shelley, D. G. Silverman, and K. H. Chon, “Statistical approach for the detection of motion/noise artifacts in photoplethysmogram,” in *IEEE International Conference on Engineering in Medicine and Biology Society*, 2011, pp. 4972–4975.
- [11] J. A. Sukor, S. Redmond, and N. Lovell, “Signal quality measures for pulse oximetry through waveform morphology analysis,” *Physiological Measurement*, vol. 32, no. 3, pp. 369–384, 2011.
- [12] P. Andersen and B. Saltin, “Maximal perfusion of skeletal muscle in man,” *The Journal of Physiology*, vol. 366, no. 1, pp. 233–249, 1985.
- [13] J. Mietus, C. Peng, I. Henry, R. Goldsmith, and A. Goldberger, “The pnnx files: re-examining a widely used heart rate variability measure,” *Heart*, vol. 88, no. 4, pp. 378–380, 2002.
- [14] J. W. Chong, D. K. Dao, S. Salehizadeh, D. D. McManus, C. E. Darling, K. H. Chon, and Y. Mendelson, “Photoplethysmograph signal reconstruction based on a novel hybrid motion artifact detection–reduction approach. part II: Motion and noise artifact removal,” *Annals of Biomedical Engineering*, pp. 1–13, 2014.
- [15] —, “Photoplethysmograph signal reconstruction based on a novel hybrid motion artifact detection–reduction approach. part I: Motion and noise artifact detection,” *Annals of Biomedical Engineering*, pp. 1–13, 2014.